E-proceedings of the 38th IAHR World Congress
September 1-6, 2019, Panama City, Panama
doi:10.3850/38WC092019-1890

NEW METHODOLOGIES IN THE TEACHING OF HYDRAULICS BASED ON EXPERIMENTATION AND CFD

PONTE, YOCH[(1)], PEHOVAZ, RICHARD[(2)] & CABRERA, JOSE[(3)]

[(1,2,3)] Hydraulic and Fluid Mechanics Laboratory, Department of Civil Engineering,
Pontificia Universidad Católica del Perú (PUCP), Lima, Perú
yponte@pucp.edu.pe; pehovaz.rp@pucp.pe; jcabrera@pucp.edu.pe

ABSTRACT

Lectures and experimental laboratories are fundamental elements for the teaching of hydraulics. The development and advance of this technology, gives us today the possibility of measuring, predicting and analyzing the behavior of a large number of hydraulic variables associated with an experiment; however, many of the hydraulics laboratories intended for teaching, do not have these facilities (e.g. PIV, LIST, ADV, Ultra-high-speed cameras, etc). In order to understand the behavior of flow patterns at different scales, this methodology has been implemented based on experimental data collection and complemented with sophisticated CFD Tools. The results of CFD models show mainly high spatial-temporal resolution hydraulic parameters, such as velocity profiles, water-air interface captures, turbulence, flow patterns, coherent turbulent structures, etc. This paper shows the results that we have obtained by complementing basic measurements of laboratory experiments with high-fidelity simulations with the use of HPC resources for five laboratory sessions and its implementation of the Open Channel Hydraulics course at Pontificia Universidad Católica del Perú.

Keywords: CFD, Hydraulics, Hydraulic laboratory, Engineering Teaching

1 INTRODUCTION

As education and technology merge, the opportunities for teaching and learning expand even more. [Xanthopoulos, 2011]. Many academic courses that teach engineering subjects have already incorporated computer-based educational tools for student use, either in the lectures or in the laboratory practices or both [Wicker, 2000]. The development and renovation of laboratory equipment as well as the limited investment for high-gamma equipment limit, sometimes, the offer that the professors of these courses can offer; however, the changing requirements of the job market for graduating engineers and engineering educators imposes the acquirement of skills that can only be learned in a laboratory setting where computational tools and modern instrumentation. On the other hand, for a teaching with a high-quality standard, not only the equipment and the computational tools required are enough; It also requires the expertise of academic members to be able to transmit and support that information in an adequate and clear manner [Knight and McDonald, 1998].

The advancement in computational power along with the user-friendly graphical user interface of Computational Fluid Dynamics (CFD) tools and High-Performance Computing (HPC) resources enable undergraduate engineering students to perform simulation analysis of flow behavior providing better understanding of fluid flow phenomenon. In contrast, the resolution and level of detail that will be required from experimentalists will even increase to catch up with the predictive capabilities of high-fidelity, multiphysics, and multiresolution simulations, help quantify their uncertainties, and develop confidence such that computational power can be used to design hydraulic engineering systems and make decisions [Sotiropoulos, 2019].

For that reason, the Laboratory of Fluid Mechanics and Hydraulics in the Department of Civil Engineering at the Pontificia Universidad Católica del Perú (PUCP), has started a pilot project in order to virtualize all the experiences of the Open Channels Hydraulics course laboratory. Familiarize the students with measurement techniques using instruments that are encountered in industry and research, to give the students experience in computer data acquisition and analysis skills, to familiarize the students the use of CFD codes, under a close guidance from a faculty member and/or a postgraduate student, expanding the students' computer application skills.

2 EXPERIMENTAL DATA COLLECTION

This study and data collection consist of 13 laboratory experiments performed in five laboratory sessions. These experiments were carried out in the Hydraulics and Fluid Mechanics Laboratory facilities at Pontificia Universidad Catolica del Peru (PUCP). Sessions and experiments are divided as follows during an academic semester:

I. First session
   E1- Permanent and uniform flow
   E2- Gradually varied flow
   E3- Rapidly Varied Flow
II. Second session
   E4- Energy
   E5- Channel bottom elevations
III. Third session
   E6- Triangular weirs
   E7- Rectangular weirs
   E8- WES (Waterways Experimental Station) type spillways
IV. Fourth session
   E9- CRUMP type spillways
   E10- Venturi flume
   E11- Parshall flume
V. Fifth session
   E12- Obstructions and pillars
   E13- Velocity distribution

All sessions are carried out in a prismatic, rectangular channel of 9x0.4x0.53m (length, width, and height) regulated by a centrifugal pump that transports up to a maximum of 50 l/s. Water levels and velocity data sets are measured in C-1 (1.5m) and C-2 (7.5m) section at longitudinal direction using Limnimeters and a Pitot-Static probe, respectively. The flow is controlled putting in service of a digital-flowmeter located before the flow enters to channel. Finally, for each experiment, a hydraulic structure associated with it will be used.

Figure 1. Experimental components, Laboratory of Hydraulics and Mechanics of Fluids, PUCP. F1-a) Rectangular channel, F1-b) Flowmeter and F1-c) Limnimeter.

This work describes the previous results for three experiments: I-E3: Rapidly Varied Flow, III-E8: WES (Waterways Experimental Station) type spillways and V-E12: Obstructions and pillars.

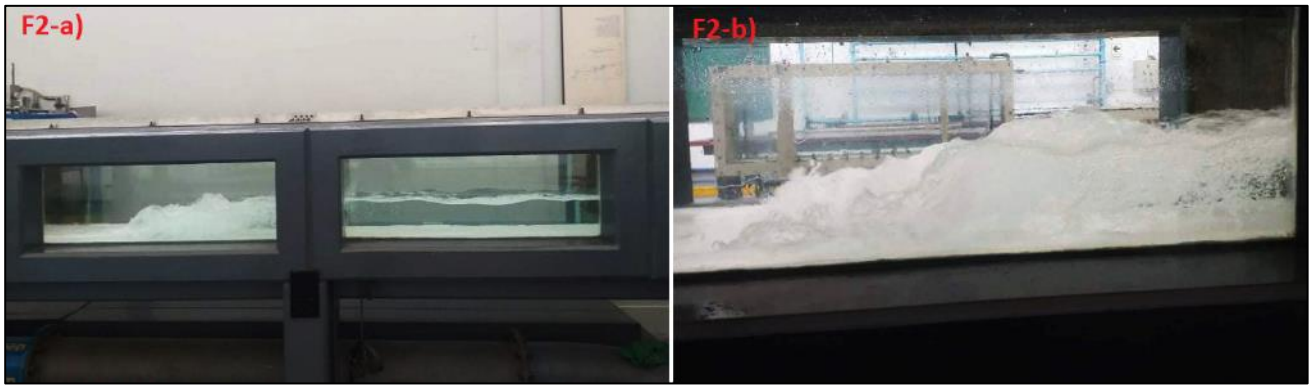

Figure 2. Case I-E3, Rapidly Varied Flow F2-a) Front view of hydraulic jump, F2-b) View of the dissipation with formation of bubbles and dissipation of energy.

Figure 3. Case III-E8: WES type spillways, F3-a) Transverse view, F3-b) Longitudinal view.

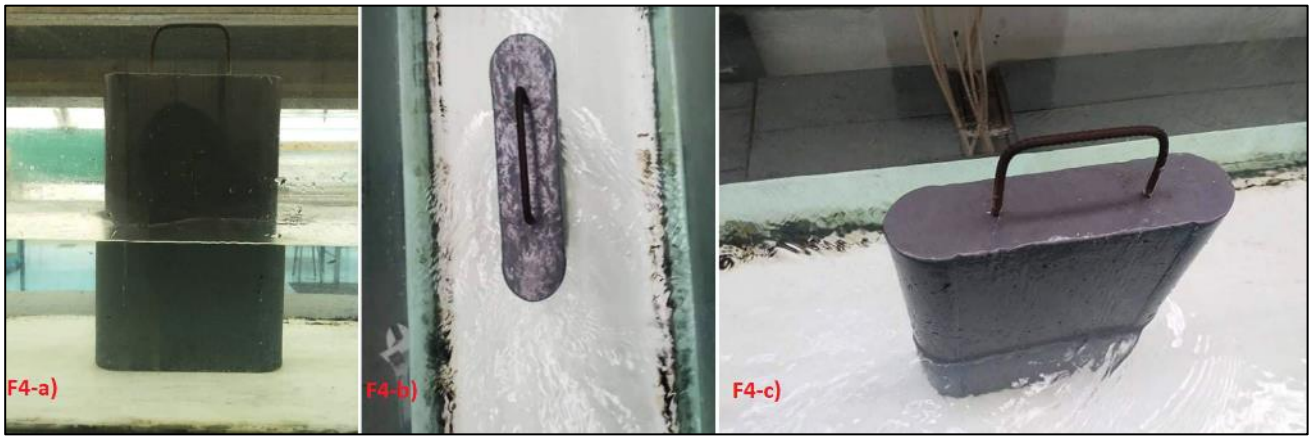

Figure 4. Case V-E12: Obstructions and pillars, F4-a) Transverse view, F4-b) Top longitudinal view and F4-c) Isometric view of the flow pattern on the pillar.

3 NUMERICAL MODEL AND COMPUTATIONAL SETUP

This study includes three simulation cases were prepared for this paper. For all cases, a three-dimensional Reynolds Averaged Navier Stokes (RANS) hydrodynamics computer model was used with a k−ω shear stress transport (SST) turbulence model [Menter, 1993]. This model is well-suited for wall bounded domains such as experimental flumes. The solution of the equations was carried out in OpenFOAM [OpenFOAM-Foundation, 2016]. OpenFOAM is an open source code software that can handle Computational Fluid Dynamics (CFD) models such as Direct Numerical Simulation (DNS), Large Eddy Simulation (LES), Detached Eddy Simulation (DES) and RANS models.

The three-dimensional RANS equations are:

$$\frac{\partial \overline{u_i}}{\partial x_i} = 0 \quad [1]$$

$$\frac{\partial \overline{u_i}}{\partial t} + \overline{u_j}\frac{\partial \overline{u_i}}{\partial x_j} = -\frac{1}{\rho}\frac{\partial \bar{p}}{\partial x_i} + \frac{1}{\rho}\frac{\partial \bar{p}}{\partial x_j}\left(2\nu\overline{s_{ji}} - \overline{u'_j u'_i}\right) \quad [2]$$

where $\overline{S_{ji}} = \frac{1}{2}\left(\frac{\partial \overline{u_j}}{\partial x_i} + \frac{\partial \overline{u_i}}{\partial x_j}\right)$. This system of equations needs to be closed by establishing an expression for the Reynolds-stress tensor $\tau_{ij} = -\rho\overline{u'_j u'_i}$. Here, a Boussinesq eddy-viscosity approximation $\tau_{ij} = \nu_t \frac{\partial \overline{u_i}}{\partial x_j}$ is used, where ν_t is the eddy viscosity (for more detail about the Boussinesq eddy-viscosity approximation, see Wilcox [1993]). The eddy viscosity is calculated using the a two-equation $k-\omega$ SST turbulence energy model [Menter, 1993]. The model computes the eddy viscosity ν_t using an equation for the turbulent kinetic energy k and the specific dissipation rate of energy ω as follows:

$$\nu_t = \frac{a_1 k}{\max(a_1\omega, SF_2)} \quad [3]$$

$$\frac{\partial k}{\partial t} + U_j \frac{\partial k}{\partial x_j} = P_k - \beta^* k\omega + \frac{\partial}{\partial x_j}\left[(\nu + \sigma_k \nu_T)\frac{\partial k}{\partial x_j}\right] \quad [4]$$

$$\frac{\partial \omega}{\partial t} + U_j \frac{\partial \omega}{\partial x_j} = \alpha S^2 - \beta\omega^2 + \frac{\partial}{\partial x_j}\left[(\nu + \sigma_\omega \nu_T)\frac{\partial \omega}{\partial x_j}\right] + 2(1-F_1)\sigma_{\omega 2}\frac{1}{\omega}\frac{\partial k}{\partial x_i}\frac{\partial \omega}{\partial x_i} \quad [5]$$

where, $S = \sqrt{2S_{ij}S_{ij}}$ is the strain rate magnitude, $a_1 = 0.31$, $\beta^* = 0.09$ and the rest of the variables are defined by the following equations:

$$P_k = \tau_{ij}\frac{\partial U_i}{\partial x_j} \quad [6]$$

$$\sigma_k = \frac{1}{F_1/\sigma_{k1} + (1-F_1)/\sigma_{k2}} \quad [7]$$

$$F_2 = \tanh\left[\left[\max\left(\frac{2\sqrt{k}}{\beta^*\omega y}, \frac{500\nu}{y^2\omega}\right)\right]^2\right] \quad [8]$$

The algorithm used to solve this system of equations (1-8) was the Semi-Implicit Method for Pressure Linked Equations (SIMPLE) algorithm. The construction of the solution matrices was carried out using the Volume of Fluid (VOF) method. The simulations were run until reaching steady state conditions (relative residuals of less than $1x10^{-3}$ for all variables U, k, ω and p). A second-order Gaussian integration numerical scheme was used to advance all terms of the system of equations in time. The interpolation schemes used from cell centers to face centers were linear central for all the gradient terms, linear upwind for all the divergence and linear corrected Laplacian terms in the system of equations.

The basic input data for mesh generation are surfaces for the experimental flume and the water elevation given as STereoLithography (STL) files for cases I-E3, III-E8 and V-E12. The procedure carried out to determine these input files is explained below.

General workflow: A background mesh with the channel dimensions of 9x0.4x0.5 m was generated. The average cell size is 1 cm, and it has much thinner cells on the channel walls. The average flow for all cases is 20 l/s.

Case I-E3: With a total of 2.8 million cells, a constant water-level of 0.45 m boundary condition was defined at inlet and a velocity magnitude of 0.25 m / s. For outlet, a pressure zerogradient and a constant water-level of 0.2 m is defined.

Case III-E8: With a total of 3.1 million cells, a constant water-level of 0.35 m boundary condition was defined at inlet and a velocity magnitude of 0.2 m / s. For outlet, a pressure zerogradient and a constant water-level of 0.04 m is defined.

Case V-E12: With a total of 2.7 million cells, a constant water-level of 0.3 m boundary condition was defined at inlet and a velocity magnitude of 0.2 m / s. For outlet, a pressure zerogradient and a constant water-level of 0.28 m is defined.

The calibration of the model was carried out by means of speed measurements made in C-1 and C-2 and in turn compared with the numerical results extracted in the same position. For cases I-E3 and III-E8, only the

results are shown in section C-1 because the Pitot-Static probe presents an unstable reading margin due to the instability of the flow and turbulence in C-2.

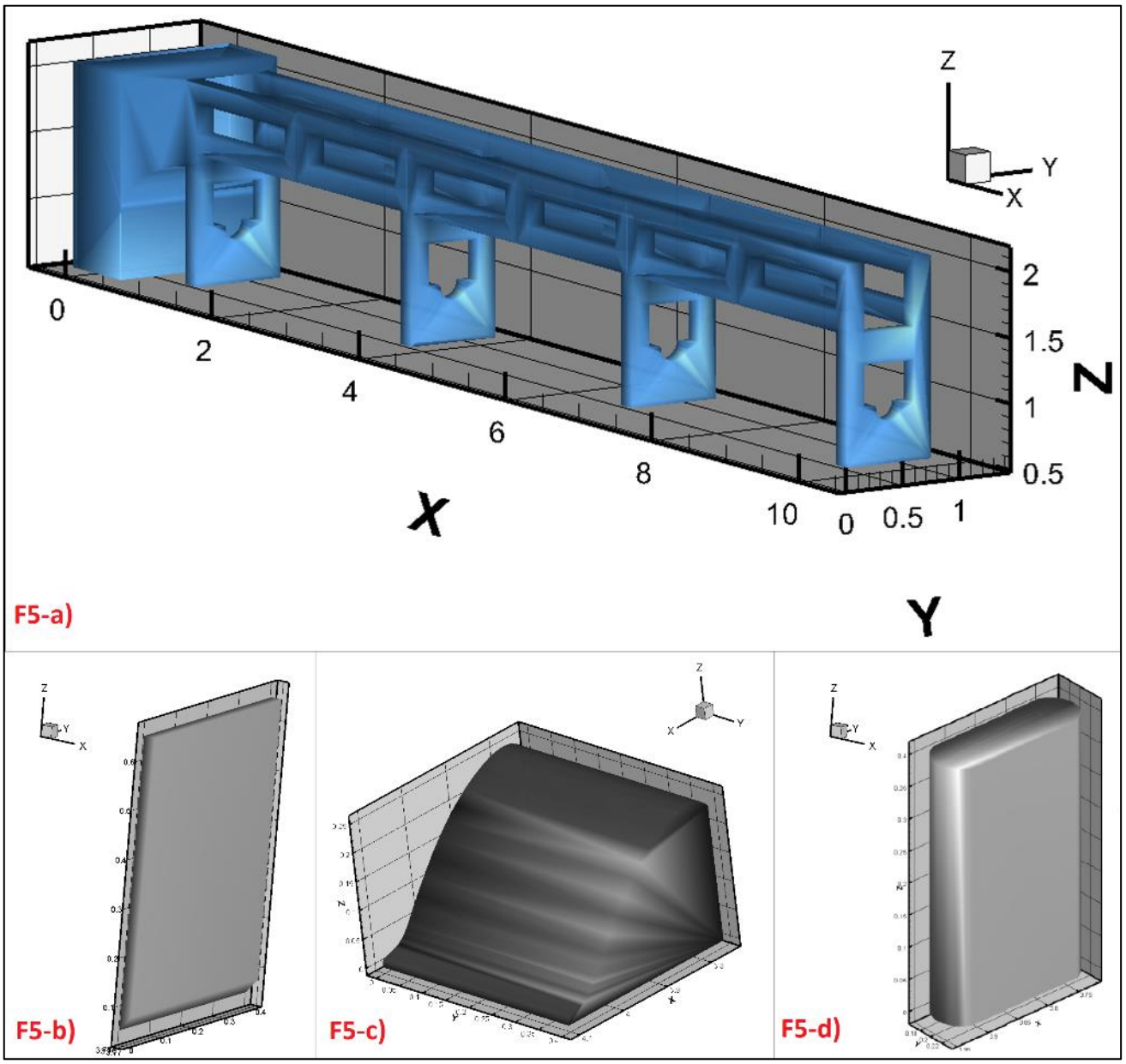

Figure 5. STLs generated for the reproduction of the 3 cases. F5-a) STL of the rectangular channel used in all simulations, F5-b) Vertical gate, used for I-E3 case. F5-c) WES Type spillway used for the III-E8 case and F5-d) Semicircular pillar used to reproduce the V-E12 case.

4 RESULTS

The results shown below show a statistical correlation between the experiences of the laboratory and the data obtained through numerical simulations. The main contributions of this simulation are the three-dimensional structure of the flow that is impossible to reproduce by means of conventional equipment in the laboratory as well as an important data base with parameters such as energy dissipation, static pressure, vorticity, etc.

The case I-E3, shows the recircular pattern of the flow caused by the vorticity and the dissipation of energy in the formation of the hydraulic jump Figure 6(a-1), also the asymmetrical structure of the flow at the outlet of the vertical gate is observed, this temporal singularity is due to the unstable nature of the flow with high Reynolds order Figure 6(a-3). The case III-E8, a uniform flow is observed before the weir and the absence of recirculation due to the absence of a hydraulic jupm, however, to maintain a high Reynolds due to the effect of the weir, it is maintained even asymmetry as in the case I-E3. The case V-E12, It shows a uniform flow along the channel,

however, the formation of a recirculatory flow to the back of the pillar is observed, further, an expansion of the velocity field in the pillar section is shown in the Figure 7(c-3).

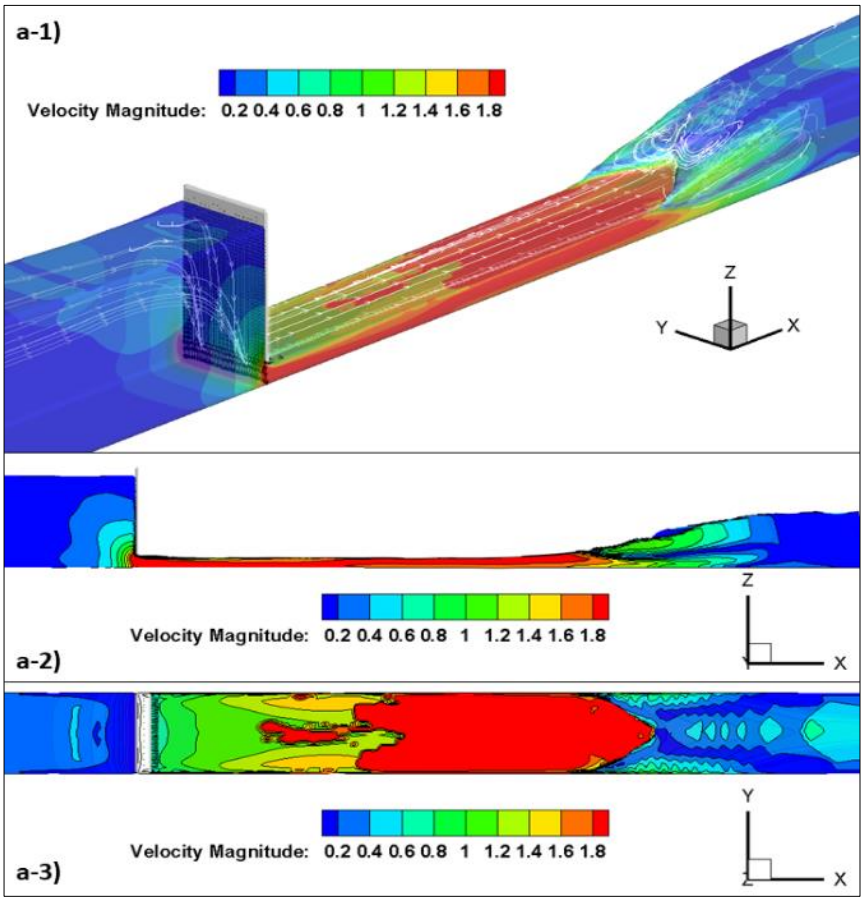

Figure 6. Results of case I-E3, colored by a color map with the magnitude of the velocity a-1) Isometric view of the flow structure and blank streamlines superimposed a-2) Transverse view and a-3) Top longitudinal view.

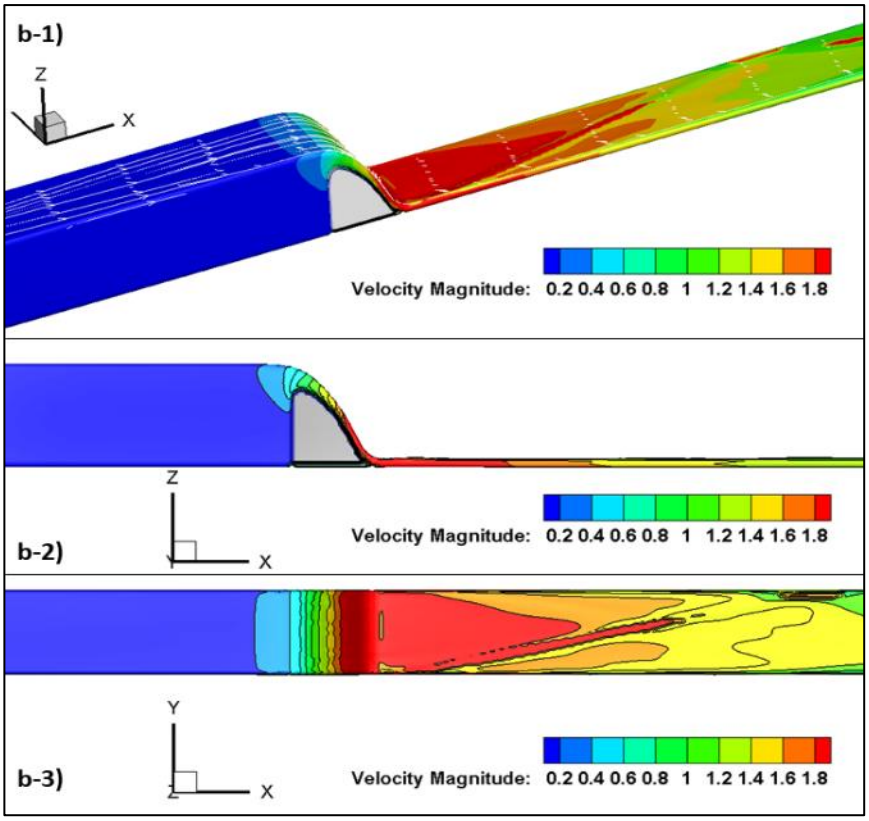

Figure 7. Results of case III-E8, colored by a color map with the magnitude of the velocity a-1) Isometric view of the flow structure and blank streamlines superimposed a-2) Transverse view and a-3) Top longitudinal view.

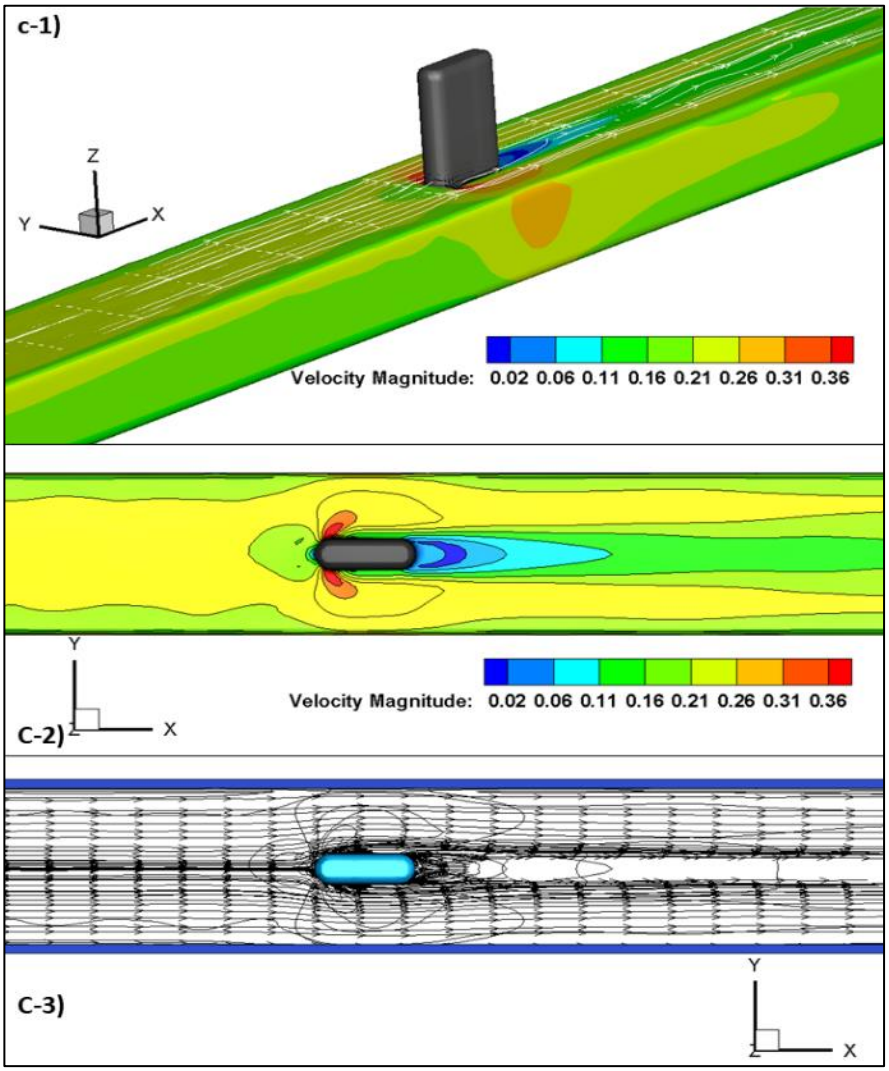

Figure 7. Results of case V-E12, colored by a color map with the magnitude of the velocity a-1) Isometric view of the flow structure and blank streamlines superimposed a-2) Transverse view and a-3) Longitudinal top view superimposed on the streamlines and the flow field.

The calibration results for these simulations were based on velocity measurements taken in the laboratory and packed with the results extracted from the numerical model. In general, the graphs in Figure 8 and Figure 9 show a remarkable correlation between both approaches.

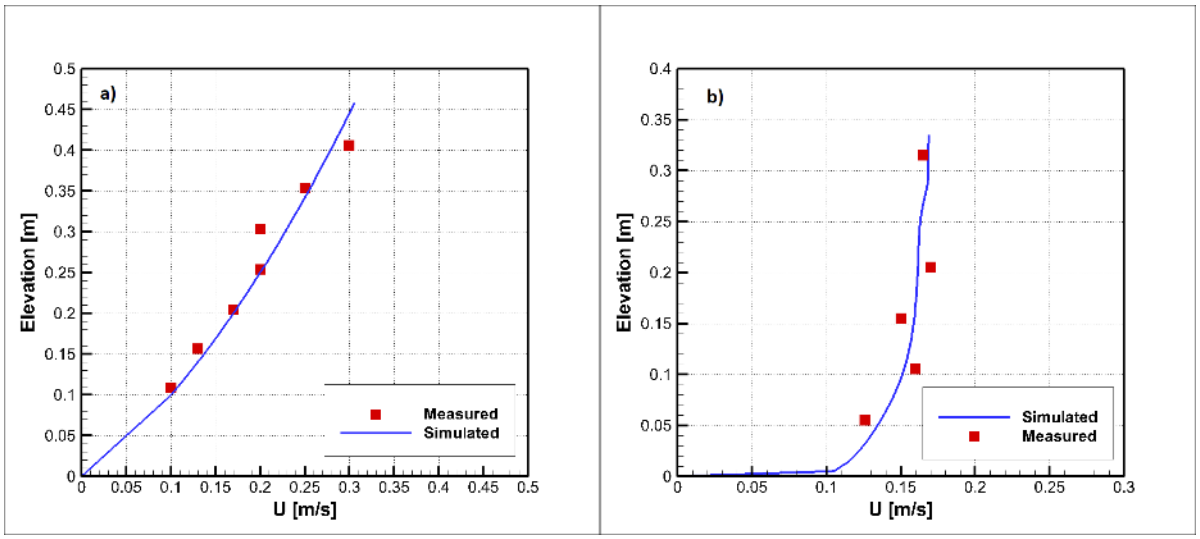

Figure 8. Comparison of the results of CFD and the data measured in the laboratory. a) I-E3 case at C-1 velocity profile, b) III-E8 case at C-1 velocity profile.

Figure 8 (a) corresponds to the results of the case I-E3, which shows a profile with a much higher slope, this because the flow has been pressurized and has worked with a water snow higher than the other cases. Figure 8 (b) corresponds to the results of case III-E8, which shows a profile with a much-smoothed slope, this because it has worked with a water level less than in the case I-E3, that the pass of flow through the weir is by overtopping.

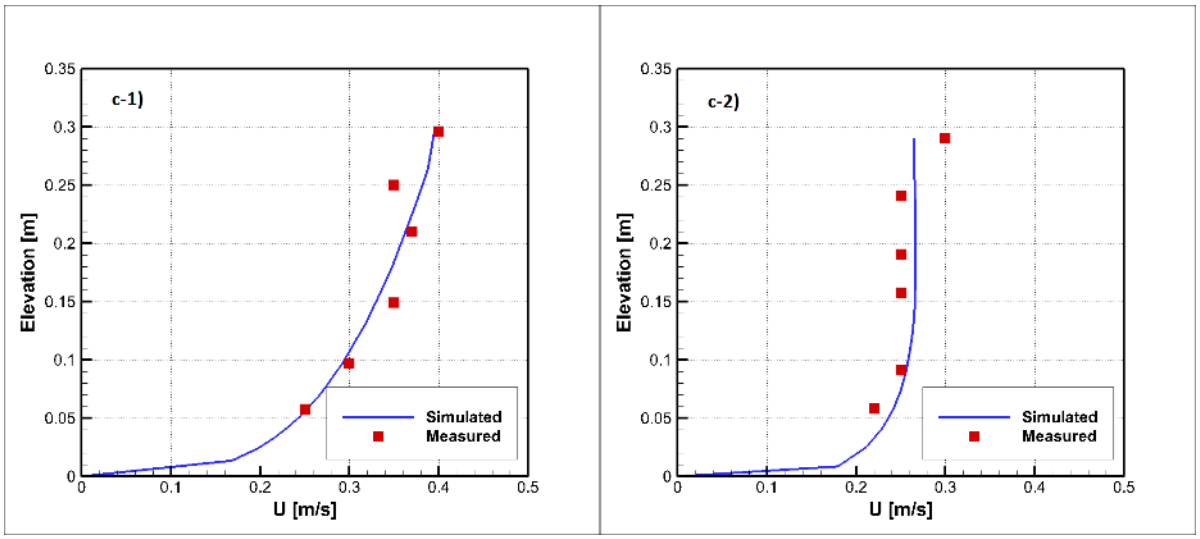

Figure 9. Comparison of the results of CFD and the data measured in the laboratory for V-E12 case. a) Velocity profile at C-1, b) Velocity profile at C-2.

Figure 9 shows the calibration results for case V-E12, where the first thing that is observed is a decrease in water level in C-1 (c-1) with respect to C-2(c-2). On the other hand, in C-1 velocity magnitud are seen much more cans than in C-2, This is because the measurements were made in the middle cross section due to the plugging of the pillar.

A complete dataset, cases, results, visualizations and HPC resources can be found on our department website: *https://paideia.pucp.edu.pe/*

5 CONCLUSIONS

Under the light of our results, we believe that the combined application of CFD, HPC resources and flipped classroom practices has the potential to provide insightful Open Channels Flo teaching and learning resources. We also believe that such application is a viable alternative to improve the course quality of academic institutions that may have resource limitations to laboratory facilities. The design of data sets and CFD skills provides students with hands-on experience, gained through an interactive and user-friendly environment, and encourages students' self-learning.

ACKNOWLEDGEMENTS

This research was conducted thanks to the funding provided by Pontificia Universidad Católica del Peru through the Innovation in University Teaching Foundation (2018-1). The authors are grateful for the support provided to carry out this research at FONDECYT-E009-2019-01 with contract number: 079-2019-FONDECYT. It would not have been possible without the experimental-data support of Anghelo Azabamba, research assistant of the Hydraulic and Fluid Mechanics Lab at PUCP.

REFERENCES

Fraser, D. M. et al. (2007) *'Enhancing the Learning of Fluid Mechanics Using Computer Simulations'*, Journal of Engineering Education, 96(4), pp. 381–388. doi: 10.1002/j.2168-9830.2007.tb00946.x.

Guessous, L. et al. (2003) '*Combining experiments with numerical simulations in the teaching of computational fluid dynamics'*, in Proceedings of the 2003 American Society for Engineering Education Annual Conference & Exposition.

Knight, C.V. and McDonald, G.H. (1998), "*Modernization of A Mechanical Engineering Laboratory Using Data Acquisition with LabVIEW*", Proceedings of the 1998 ASEE Annual Conference & Exposition, Seattle, Washington, Session 2266, 1998, pp. 1-13.

Menter, F. (1993), *Zonal two equation k- turbulence models for aerodynamic flows*, AIAA 24th Fluid Dynamics Conference.

OpenFOAM-Foundation (2016), OpenFOAM, *The Open Source CFD Toolbox User Guide*, OpenFOAM Foundation.

Ronald Gutierrez et al. (2017). *Combined application of cfd and flipped classroom practices in improving knowledge acqusition for an undergraduate water resources engineering related course,* Proceedings of the 33rd International Academic Conference, Vienna, DOI: 10.20472/IAC.2017.33.

Wicker, R.B. and Loya, H.I. (2000), "*A Vision-based Experiment for Mechanical Engineering Laboratory Courses*", Intern. J. Engineering Education, Vol. 16, No. 3, pp. 193-201.

Wilcox, D. C. (1993), *Turbulence Modeling for CFD*, DCW Industries Inc., La Cañada, CA.

Xanthopoulos, E. I. et al. (2011). Use of virtual instrumentation and computational fluid dynamics in an undergraduate research project, in 7th GRACM International Congress on Computational Mechanics.

Sotiropoulos, Fotis et al. (2019). *Hydraulic Engineering in the Era of Big Data and Extreme Computing: Can Computers Simulate River Turbulence?* Journal of Hydraulic Engineering, doi: 10.1061/(ASCE)HY.1943-7900.0001594.